Published in final edited form as:
Invest Ophthalmol Vis Sci. 2009 August ; 50(8): 3589–3595. doi:10.1167/iovs.08-3336.

Formation of all-*trans* Retinol after Visual Pigment Bleaching in Mouse Photoreceptors

Chunhe Chen[1], **Lorie R. Blakeley**[1], and **Yiannis Koutalos**[1,2]

[1]Department of Ophthalmology, Medical University of South Carolina, Charleston, South Carolina.

[2]Departments of Neurosciences, Medical University of South Carolina, Charleston, South Carolina.

Abstract

PURPOSE—To test whether the formation of all-*trans* retinol limits the regeneration of the visual pigment. all-*trans* retinol is formed after visual pigment bleaching through the reduction of all-*trans* retinal in a reaction involving NADPH. This reduction begins the recycling of the chromophore for the regeneration of the visual pigment.

METHODS—Experiments were performed with dark-adapted, isolated retinas and isolated photoreceptor cells from wild-type and $Nrl^{-/-}$ mice. The photoreceptors of $Nrl^{-/-}$ mice are conelike and contain only cone pigments. The formation of all-*trans* retinol after pigment bleaching was measured by quantitative HPLC of retinoids extracted from isolated retinas and by imaging the fluorescence of retinol in photoreceptor outer segments. Experiments were performed at 37°C.

RESULTS—In rods, the formation of all-*trans* retinol proceeded with first-order kinetics, with a rate constant of 0.06 ± 0.02 minute^{-1}, significantly faster than the reported rate constant for rhodopsin regeneration. In $Nrl^{-/-}$ photoreceptors, the formation of all-*trans* retinol occurred at least 100 times faster than in rods. For both cell types, the fraction of all-*trans* retinal converted to all-*trans* retinol at equilibrium is ~0.8, indicating the presence of a similar fraction of reduced NADPH.

CONCLUSIONS—Formation of all-*trans* retinol does not limit the regeneration of bleached visual pigment. Formation of all-*trans* retinol in the cone-like $Nrl^{-/-}$ photoreceptors is much faster than in rods, consistent with a faster regeneration of the visual pigment after bleaching. Different types of photoreceptors contain a comparable fraction of reduced NADPH to drive the reduction of all-*trans* retinal.

Vision is initiated by the absorption of light by the visual pigment present in the outer segments of the rod and cone photoreceptor cells in the retina. In both cell types, the first step in the detection of light is the photoisomerization of the retinyl chromophore of the visual pigment from 11-*cis* to all-*trans*.[1,2] This isomerization of the chromophore bleaches the pigment, necessitating its regeneration with fresh 11-*cis* retinal. The production of 11-*cis* retinal includes the recycling of the all-*trans* chromophore of the bleached pigment through a series of reactions called the visual cycle.[3–5] These reactions begin in the outer segment with the release of all-*trans* retinal from the photoactivated pigment and its reduction to all-*trans* retinol by retinol dehydrogenase in a reaction using NADPH.[6] The all-*trans* retinol is then transferred from outer segments to the adjacent retinal pigment epithelial cells,[7] where it is esterified to form retinyl ester.[8,9] The ester is converted to 11-*cis* retinol,[10–13] which is then oxidized to 11-*cis* retinal.

Corresponding author: Yiannis Koutalos, Department of Ophthalmology, Medical University of South Carolina, 167 Ashley Avenue, Charleston, SC 29425; koutalo@musc.edu.

Disclosure: **C. Chen**, None; **L.R. Blakeley**, None; **Y. Koutalos**, None

[14] Studies of cone-dominant ground squirrel and chicken retinas have provided evidence of the presence of an additional visual cycle used by cones.[15–17] Continuous vision depends on the regeneration of the visual pigment and defects in the processing of the chromophore through the reactions of the visual cycle are responsible for a wide range of visual defects.[3,18]

Extensive studies using whole eyes have argued for the presence of two slow steps in the operation of the mouse visual cycle: the formation of all-*trans* retinol and the isomerization of all-*trans* retinyl ester.[19–21] Although the formation of all-*trans* retinol has been characterized in detail in amphibian photoreceptors,[22–24] these results cannot provide a quantitative insight into the operation of the mouse visual cycle because of critical species differences, such as body temperature. Therefore, we undertook the measurement of the kinetics of all-*trans* retinol formation in mouse photoreceptors by HPLC of retinoid extracts and fluorescence imaging. In our results, all-*trans* retinol formation was not the slowest step in the mouse visual cycle, which supports the notion that the isomerization of retinyl esters is the slowest step.[20,21] Throughout the text, unqualified retinal and retinol refer to the all-*trans* isomers.

METHODS

Wild-type mice (C57BL/6J) were from The Jackson Laboratory (Bar Harbor, ME). *Rpe65*$^{-/-}$ and *Nrl*$^{-/-}$ mice were from established colonies at the Medical University of South Carolina. *Rpe65*$^{-/-}$ mice lack the 11-*cis* retinal chromophore[25] and *Nrl*$^{-/-}$ mice lack Nrl, a transcription factor necessary for rod photoreceptor development.[26] All animal procedures were performed in accordance with protocols approved by the Institutional Animal Care and Use Committee of the Medical University of South Carolina, and the protocol adhered to the ARVO Statement for the Use of Animals in Ophthalmic and Vision Research. Animals were kept in cyclic light, 12-hour light cycle (0600–1800 hours). For the experiments, we used 2- to 3-month-old animals. In animals between the ages of 2 and 3 months, we have not observed significant age-dependent differences in the kinetics of retinol formation. We have not been able to obtain reliable results from *Nrl*$^{-/-}$ mice older than 3 months, presumably because of the deterioration of their retinas with age.[27] Animals were dark-adapted overnight and killed under dim red light. The retinas were excised under either dim red or infrared light in mammalian Ringer's (in mM: 130 NaCl, 5 KCl, 0.5 $MgCl_2$, 2 $CaCl_2$, 25 hemisodium-HEPES, and 5 glucose [pH 7.40]). All reagents were of analytical grade.

For HPLC measurements, isolated retinas were incubated at 37°C in bicarbonate Ringer's (in mM: 94 NaCl, 5 KCl, 0.5 $MgCl_2$, 2 $CaCl_2$, 25 hemisodium-HEPES, 24 NaHCO3, and 5 glucose, [pH 7.40]) gassed with 95% O_2 and 5% CO_2 (at 1 atm) to maintain the pH. Virtually identical results were obtained when the mammalian Ringer's was used, without bicarbonate and without gassing. For these experiments, the retinas were fully separated from the pigment epithelium. This separation eliminates the transfer of retinol from the photoreceptors to the pigment epithelium and results in its accumulation in the rod outer segments.[28,29] In this way, the formation of retinol can be studied without interference by the subsequent reactions of the visual cycle. Retinoids were extracted at different times after bleaching the retina and processed for HPLC (Waters Corp., Milford, MA). UV light (10 seconds of 360 nm light from a UVGL-25, light flux 1.4 mW cm^{-2}) was used for bleaching *Nrl*$^{-/-}$ mouse retinas; long-wavelength light (1 minute; >530 nm from a 150-W halogen lamp illuminator) was used for bleaching wild-type mouse retinas. For retinoid extraction, essentially the same procedures outlined previously[29] were followed. The only difference was the mobile phase, which here consisted of hexanes (HPLC grade), ethyl acetate, octanol, and dioxane in 91.8:6.6:0.8:0.8 ratios.[19] The relative amount of a retinoid in the sample was calculated from the area under its peak, and its extinction coefficient. The fraction of all-*trans* retinol was calculated from the relative amounts and used as the measure of all-*trans* retinol formation.[29] In this way, measurement of the kinetics of retinol formation is not affected by the different number of rod

outer segments present in individual preparations. One wild-type and four $Nrl^{-/-}$ retinas were used for each experimental determination, as these numbers provided adequate material for analysis. It was necessary to use more $Nrl^{-/-}$ retinas, because one $Nrl^{-/-}$ retina contains ~15% of visual pigment compared with the wild-type.[27]

Retinol fluorescence measurements were performed with slices from wild-type and $Rpe65^{-/-}$ retinas and isolated cells from wildtype and $Nrl^{-/-}$ retinas. Slices of retinas were prepared as described[23] and placed in a chamber that fit on the microscope stage. Isolated photoreceptor cells were obtained by chopping the retina with a razor blade in a dish coated with an elastomer (Sylgard; Dow Corning, Midland, MI) and placed in 100-μL chambers that fit on the microscope stage. To keep the cells in place during the experiment, the bottoms of the chambers were coated with 0.01% polylysine or polyornithine solutions (Sigma-Aldrich, St. Louis, MO). Fluorescence imaging experiments were performed on the stage of an inverted microscope (Axiovert 100; Carl Zeiss Meditec, Thorn-wood, NY), with 360 nm excitation and >420 nm emission.[29] For slices, one of two objective lenses was used (a water-immersion 40× Achroplan [NA = 0.8], and for isolated cells an oil immersion 40× Plan Neofluar [NA = 1.3]; both by Carl Zeiss Meditec). The experiments were performed at 37°C. To maintain the higher temperature, we heated the microscope stage and the oil-immersion objective (Warner Instruments, Hamden, CT). Fluorescence images were acquired at different times after bleaching a slice or an isolated cell. For bleaching, long-wavelength light (1 minute; >530 nm from a 150-W halogen lamp illuminator) and 360-nm light (10 seconds from the Xenon arc lamp of the imaging system; flux 1 mW cm^{-2}) were used for wild-type and $Nrl^{-/-}$ tissues, respectively. Fluorescence intensity was measured over defined regions of interest (ROIs) in the outer segments and background. In experiments with slices, after correcting for background, the fluorescence intensities were divided by the initial value before bleaching. In experiments with isolated cells, after correction for the background, the initial value before bleaching was subtracted from all subsequent values to obtain the fluorescence due to retinol; retinol fluorescence was then converted to retinol concentration (in mM) through a calibration procedure using hexane/chloroform droplets containing a concentration of 1.5 mM all-*trans* retinol.[29]

To describe and compare the measurements of retinol across techniques and cell types, we approximated the formation and elimination of retinol as two separate first-order processes:

$$\text{metarhodopsin} \xrightarrow{f_1} \text{retinol} \xrightarrow{f_2} \text{bulk solution} \tag{1}$$

with f_1 and f_2 the apparent rate constants of formation and elimination, respectively. Hereafter, we will refer to f_1 and f_2 simply as rates. The generation of metarhodopsin from rhodopsin by light was assumed to be much faster than the subsequent processes. This assumption is clearly not valid for the experiments with $Nrl^{-/-}$ cells, in which case the formation kinetics are not fully resolved. For the measurements of whole retinas and retina slices, the outer segments were closely packed together resulting in a small surface-to-volume ratio, so there was virtually no elimination of retinol, and $f_2 \approx 0$. In that case, the concentration of retinol *ROL* as a function of time *t* after bleaching is given by

$$ROL = C_0 \cdot (1 - e^{-f_1 \cdot t}) \tag{2}$$

where C_0 is the concentration that retinol attains at steady state, long after bleaching. Well after bleaching, all the all-*trans* retinal chromophore has been released from metarhodopsin, and a concentration C_0 has been converted to retinol. So, C_0 is the concentration of retinol at equilibrium with retinal. As all chromophore is derived from the bleaching of rhodopsin, the

total chromophore concentration is the same as that of bleached rhodopsin concentration, P_0. At equilibrium,

$$C_0 = \beta \cdot P_0 \tag{3}$$

with $\beta \approx 0.8$ based on the known thermodynamics of the reaction.[29]

In the case of isolated photoreceptor cells, the large surface-to-volume ratio allows for the faster elimination of retinol, and $f_2 > 0$. In that case,[22]

$$ROL = \frac{f_1 \cdot C_0}{f_1 - f_2} \cdot (e^{-f_2 \cdot t} - e^{-f_1 \cdot t}) \tag{4}$$

In general, the parameters C_0 and f_1 in equation 4 may not be the same as in equation 2. One special case for which the parameters are the same is when retinal is in rapid equilibrium with retinol. In that case, f_1 is the actual rate of all-*trans* retinal release from metarhodopsin, and f_2 is the actual rate of all-*trans* retinol elimination from the outer segment. It should be kept in mind that in general the assignment of physical meaning to the parameters appearing in equation 4 is model-dependent.

Parameters were determined by least-squares fits (Kaleidagraph; Synergy Software, Reading, PA). Errors for parameters were obtained from the curve fits.

RESULTS

Kinetics of all-*trans* Retinol Formation in Mouse Rod Photoreceptors

Exposure of vertebrate photoreceptor cells to light results in the formation of retinol in the photoreceptor outer segments. In isolated retinas, separated from the retinal pigment epithelium, the all-*trans* retinol formed after light exposure cannot be transported away by carriers. Furthermore, the closely packed rod outer segments result in a low surface to volume ratio slowing down the escape of retinol to the bulk solution, so that it accumulates in the outer segment membranes. Figure 1 presents the results obtained under such conditions. Figure 1A shows the chromatographic profiles of retinoids extracted from wild-type mouse retinas incubated at 37°C for different times after light exposure. In the dark (trace a), almost all of the chromophore was in the 11-*cis* configuration. After bleaching the retina with >530 nm light for 1 minute, almost all the 11-*cis* retinal chromophore was isomerized to all-*trans* (trace b), meaning that all the rhodopsin was bleached. Subsequently, all-*trans* retinal was reduced to all-*trans* retinol, which accumulated in the retina (traces c and d). From such data we obtained the increase in the fraction of retinol with time after bleaching (Fig. 1B). We converted the fraction of retinol to its corresponding concentration in the outer segment (Fig. 1B, right *y*-axis), using a rhodopsin concentration of 3 mM for mouse rods.[30] The overall rate of formation, obtained by fitting the data with equation 2, is $f_1 = 0.04 \pm 0.01$ minute^{-1}, and the fraction of retinal chromophore converted to retinol at equilibrium is 0.82 ± 0.04, which corresponds to a retinol concentration of 2.5 mM (0.82×3). Similar results were obtained by using the fluorescence of retinol to monitor its accumulation in retina slices (Fig. 2). As in the case of the whole isolated retina, retinol accumulated after light exposure with a rate constant of 0.06 ± 0.01 minute^{-1}, in reasonable agreement with the time course measured from whole retinas with HPLC. Figure 2 also shows that, as expected, there was no fluorescence increase in the rod outer segments of retinas from *Rpe65*$^{-/-}$ mice (filled diamonds), which lack the 11-*cis* retinal chromophore,[25] in agreement with the published results at room temperature.[23]

A disadvantage of the slice preparation is its limited resolution: First, it does not provide information at the level of the single outer segment and second, because the exact tissue thickness from which fluorescence is collected is not known, it is not possible to convert fluorescence intensities to retinol concentration. Therefore, we undertook experiments with isolated rod photoreceptor cells (Fig. 3A). The bleaching of rhodopsin results in an increase in retinol fluorescence in the outer segment, which is followed by a decrease, as retinol escapes to the bulk solution. Of importance, retinol fluorescence increases uniformly in the outer segment, without any evidence of the gradients observed in salamander and gecko photoreceptors.[22,24,31] We can then convert the fluorescence of retinol to a single outer segment concentration using a calibration procedure with retinol-containing droplets.[29] This conversion allows the direct comparison of the fluorescence intensity data with the biochemical extraction data. The kinetics of retinol formation (average from $n = 13$ cells) are shown in Figure 3B. Fitting the data with equation 4 gives $f_1 = 0.06 \pm 0.02$ minute^{-1}, $f_2 = 0.024 \pm 0.009$ minute^{-1}, and $C_0 = 2.5 \pm 0.7$ mM. The rate of formation f_1 is in good agreement with the extraction and slice data, and amplitude C_0 is the same as the one obtained from the extraction data at time points long after bleaching. Overall, the results obtained with the three different preparations (whole retina, slice, and isolated cells), which were subjected to vastly different levels of physical strain, are in good agreement. In addition, our results are in good agreement with the measurements of all-*trans* retinal clearance after bleaching from experiments with whole animals (time constant of 15 minutes,[20] corresponding to a rate of 0.07 minute^{-1}). Thus, it is very unlikely that our measurements were affected by damage to the photoreceptors arising from the separation of the retina from the retinal pigment epithelium.

Kinetics of all-*trans* Retinol Formation in Conelike *Nrl*$^{-/-}$ Photoreceptors

Cone photoreceptors operate under bright light conditions, necessitating the rapid regeneration of the visual pigment. We selected the retinas of the *Nrl*$^{-/-}$ mice to study the formation of retinol in cone photoreceptors. The cone pigments found in the *Nrl*$^{-/-}$ retina are the same as in wild-type, a short-wavelength ($\lambda_{max} \sim 360$ nm) and a middle-wavelength ($\lambda_{max} \sim 510$ nm) sensitive,[32] with most of the light sensitivity being due to the short-wavelength sensitive one. Compared with wild-type, retinol formed much faster in the *Nrl*$^{-/-}$ retinas (Fig. 4). Figure 4A shows chromatograms of retinoids extracted from the *Nrl*$^{-/-}$ mouse retinas at different times after light exposure. Most of the retinoid in dark-adapted retinas was 11-*cis* retinal (trace a), though a substantial amount of all-*trans* retinoids comprising ~10% of the total pool was present as well, in agreement with previous results.[33,34] *Nrl*$^{-/-}$ retinas contain rosettes and whorls,[26] so that, after their separation from the rest of the eyecup, the retinas may still carry a significant contamination of retinal pigment epithelial cells. Because of the possibility of such contamination, we cannot readily conclude from our data that the all-*trans* retinoid pool was part of the retina and not a retinal pigment epithelium contaminant. Exposure to >530 nm light for 1 minute did not appreciably change the retinoid profile (trace b). We would have expected this light exposure to bleach the middle-wavelength sensitive cone pigment, but as this pigment constitutes only a small portion of the total pigment, the change in the all-*trans* retinoid pool may be below the resolution of our measurements. Exposure of a retina to 10 seconds of 360 nm light converts 50% to 60% of the 11-*cis* retinal to all-*trans* (trace c), consistent with most of the light sensitivity being due to a short-wave-length pigment. One reason for the partial conversion of 11-*cis* to all-*trans* is likely to be photoreversal of the metaproducts during the light exposure because of the overlap in their absorbance with that of the dark state of the pigment. In the case of wild-type rods containing rhodopsin, this photoreversal can be largely avoided by taking advantage of the blue-shifted spectra of the metaproducts compared with rhodopsin[35] and using long-wavelength light for bleaching. For the short-wavelength-sensitive cone pigment, however, its metaproducts are red-shifted,[36] making photoreversal difficult to avoid. After light exposure, all-*trans* retinal is swiftly converted to all-*trans* retinol (trace d), reaching within 5 minutes a fraction of 0.76 ± 0.02 that

remains stable for at least 1 hour (Fig. 4B). Fitting these data with equation 2 gives a rate of retinol formation of $f_1 = 6.8 \pm 1.9$ minutes^{-1} and a fraction of retinal converted to retinol at an equilibrium of $\beta = 0.77 \pm 0.03$. With a bleaching of ~60% of visual pigment by the 10-second UV exposure and an outer segment pigment concentration in cones of 3 mM,[27,37] this fraction of retinol corresponds to an outer segment concentration of $C_0 = 1.4$ mM ($0.77 \times 0.6 \times 3$ mM). The value of the fraction of retinal converted to retinol at thermodynamic equilibrium in *Nrl*$^{-/-}$ cells is essentially the same as for rods, ~0.8.

We did not attempt to perform fluorescence measurements of retinol formation in slices from *Nrl*$^{-/-}$ retinas, as these retinas include rosettes and whorls that compromise the proper stacking of the retina layers. We performed fluorescence imaging experiments with isolated cells (Fig. 5). After the cell was bleached with 10 seconds of 360-nm light, the retinol outer segment concentration first increased rapidly and then decreased in the course of a few minutes as retinol escaped into the bulk solution. Fluorescence intensities were converted to retinol concentrations and plotted as a function of time after bleaching (Fig. 5B; average from $n = 6$ cells). The data were fitted with equation 4, giving $f_1 = 19.5 \pm 5.9$ minutes^{-1}, $f_2 = 0.15 \pm 0.01$ minute^{-1}, and $C_0 = 1.65 \pm 0.04$ mM. The significant discrepancy, of approximately threefold, in the rate of formation obtained from whole retinas (6.8 minutes^{-1}) compared with that from isolated cells (19.5 minutes^{-1}) was probably due to the kinetics of formation being somewhat faster than the resolution of our measurements. The amplitude C_0 is in reasonable agreement with the one obtained from whole retinas when we take into account the partial conversion of 11-*cis* chromophore to all-*trans* by the bleaching light.

DISCUSSION

In our experiments, the formation of retinol in mouse rod outer segments proceeded at a rate of 0.06 ± 0.02 minute^{-1}, corresponding to a time constant of ~17 minutes. This rate was much faster than the regeneration rate of rhodopsin in the C57BL/6 mice used in our experiments, for which rhodopsin regeneration was less than 50% complete by 90 minutes.[38,39] The rate was also faster than the rate of rhodopsin regeneration in 129/sv mice (time constant of 30 minutes[20]). Therefore, the formation of retinol is not the slowest step in the mouse visual cycle (see also Ref. 21), and the recycled chromophore can contribute significantly to the retinoid pool used for the generation of rhodopsin. This result is in contrast to the previous proposal that the reduction of retinal to retinol limits the rate of rhodopsin regeneration in mice.[19] That proposal was based on the observation that light exposure of whole eyes results in accumulation of all-*trans* retinal but not of all-*trans* retinol in the retina. However, the all-*trans* retinal measured in those experiments may not have been available for reduction, as it could still be bound to photoactivated rhodopsin. The lack of all-*trans* retinol accumulation could be due to its rapid transfer to the retinal pigment epithelium. Our experiments avoided interference from subsequent reactions by measuring retinol formation directly in isolated retinas and photoreceptors. More recent investigations argued that there are two slow steps in the mouse visual cycle, reduction of all-*trans* retinal and isomerization of all-*trans* retinyl ester, because these two substances accumulated and decayed slowly during recovery from bleaching.[20] Additional experiments have further suggested that the reduction of all-*trans* retinal is faster than other steps in the visual cycle.[21] By establishing that the formation of retinol is not limiting, our results support the isomerization of the retinyl ester being the slowest step in the mouse visual cycle.[20,21] If we extrapolate to the human situation, however, rhodopsin regeneration is complete within 15 to 20 minutes (Figs. 9, 10 in Ref. 3), which is significantly faster than the retinol formation we have measured. A possible explanation is that there are important metabolic differences between mouse and human rods, and the latter can reduce all-*trans* retinal faster. Alternatively, in humans, the existing retinal pigment epithelial stores and the circulation can rapidly supply the retinoid needed for regeneration without need for the recycled chromophore.

The overall rate of formation of retinol is much slower than the reported rate of retinal release from the bleached pigment, which is ~0.3 minute^{-1} (measured at 35°C and pH of 6.5; see Fig. 2B in Ref. 40). In the living cell, however, the release of retinal may be slowed down by the binding of arrestin to photoactivated and phosphorylated rhodopsin.[41] Moreover, retinal may not become readily available for reduction, as it may accumulate in the disc lumen, forming a Schiff base with phosphatidylethanolamine and depend on the ABCR protein to be transported to the cytosol.[42–44] The availability of NADPH and the catalytic rate of retinol dehydrogenase could also limit the generation of retinol. In view of this complexity, it is not surprising that the experimental data from slices and isolated cells indicate the presence of two phases. The rapid phase is not well resolved in the measurements from whole retinas (perhaps because of the underestimation of the retinol fraction at early times; see the Methods section), but it has been observed in salamander and frog photoreceptors.[23,24] The rapid formation of retinol suggests that there is a rapid component of retinal release, and, moreover, there is sufficient NADPH present to convert this rapidly released retinal to retinol. The secondary, slower component of retinol concentration increase may be due to a variety of factors, such as a slower component of retinal release or limitations in the supply of NADPH. At this stage, our experiments cannot separate the contributions from all these different physical reactions, and we have approximated the overall formation of retinol with first order kinetics.

The rate of retinol formation in *Nrl*$^{-/-}$ cells is at least 100× higher than in wild-type rods. Such a high rate requires both a rapid release of all-*trans* retinal from the photoactivated cone pigment, and a rapid reduction by the retinol dehydrogenase. The lifetime of the short-wavelength cone pigment photointermediates is known to be in the order of seconds[45] and direct measurements of retinal release from a homologous cone pigment give a very fast time constant as well (Kuemmel CM, et al. *IOVS* 2008;49:ARVO E-Abstract 1554). As for the reduction reaction, the retinol dehydrogenase activity in cones is much greater than in rods, [46] while the supply of NADPH is unlikely to be limiting, as *Nrl*$^{-/-}$ cells (and cones in general) have a much smaller outer segment volume than rods[27] and contain a much smaller amount of retinyl chromophore that they must reduce. As with rods, the rate of retinol formation is much faster than the reported rate of cone pigment regeneration in *Nrl*$^{-/-}$ retinas, in which 11-*cis* retinal levels recover to ~50% of prebleach levels after 30 minutes.[34]

The fraction of chromophore converted to retinol at thermodynamic equilibrium with retinal is very similar, ~0.8, across cell types and species, including frog,[29] suggesting that cellular metabolic activity sets the fraction of outer segment NADPH to comparable levels. An intriguing explanation for this similarity would be the operation of a homeostatic mechanism.

In summary, we characterized the formation of retinol in mouse rod and cone photoreceptors. We found that, in both cell types, retinol formation occurred significantly faster than the reported rates for pigment regeneration. The generation of retinol proceeded at least 100× faster in cones than in rods, consistent with the overall need to regenerate the visual pigment faster in cones, so that the cells can operate continuously under bright light conditions. The fraction of NADPH in cone outer segments is similar to that of rods, pointing to a regulation of the metabolic pathways that provide the needed reducing equivalents.

Acknowledgments

The authors thank Mas Kono and Rosalie Crouch for helpful discussions, Patrice Goletz for breeding the *Nrl*$^{-/-}$ and *Rpe65*$^{-/-}$ mice, and Professor Crouch for providing us with access to HPLC equipment and with the *Nrl*$^{-/-}$ and *Rpe65*$^{-/-}$ mice.

Supported by National Institutes of Health (NIH) Grants EY04939 (Rosalie Crouch), EY14850 (YK), MUSC University Research Council Grant 29910 (YK), and an unrestricted grant to MUSC Storm Eye Institute from Research to Prevent Blindness, Inc., New York, NY. Mice were housed in a facility constructed with support from NIH Grant C06 RR015455 from the Extramural Research Facilities Program of the National Center for Research Resources.

References

1. Ebrey T, Koutalos Y. Vertebrate photoreceptors. Prog Retin Eye Res 2001;20:49–94. [PubMed: 11070368]
2. Palczewski K. G protein-coupled receptor rhodopsin. Annu Rev Biochem 2006;75:743–767. [PubMed: 16756510]
3. Lamb TD, Pugh EN Jr. Dark adaptation and the retinoid cycle of vision. Prog Retin Eye Res 2004;23:307–380. [PubMed: 15177205]
4. Saari JC. Biochemistry of visual pigment regeneration: the Friedenwald lecture. Invest Ophthalmol Vis Sci 2000;41:337–348. [PubMed: 10670460]
5. Travis GH, Golczak M, Moise AR, Palczewski K. Diseases caused by defects in the visual cycle: retinoids as potential therapeutic agents. Annu Rev Pharmacol Toxicol 2007;47:469–512. [PubMed: 16968212]
6. Futterman S, Hendrickson A, Bishop PE, Rollins MH, Vacano E. Metabolism of glucose and reduction of retinaldehyde in retinal photoreceptors. J Neurochem 1970;17:149–156. [PubMed: 4395446]
7. Okajima TI, Pepperberg DR, Ripps H, Wiggert B, Chader GJ. Interphotoreceptor retinoid-binding protein: role in delivery of retinol to the pigment epithelium. Exp Eye Res 1989;49:629–644. [PubMed: 2509230]
8. Saari JC, Bredberg DL, Farrell DF. Retinol esterification in bovine retinal pigment epithelium: reversibility of lecithin:retinol acyltransferase. Biochemical J 1993;291:697–700.
9. Batten ML, Imanishi Y, Maeda T, et al. Lecithin-retinol acyltransferase is essential for accumulation of all-trans-retinyl esters in the eye and in the liver. J Biol Chem 2004;279:10422–10432. [PubMed: 14684738]
10. Bernstein PS, Rando RR. In vivo isomerization of all-trans- to 11-cis-retinoids in the eye occurs at the alcohol oxidation state. Biochemistry 1986;25:6473–6478. [PubMed: 3491624]
11. Jin M, Li S, Moghrabi WN, Sun H, Travis GH. Rpe65 is the retinoid isomerase in bovine retinal pigment epithelium. Cell 2005;122:449–459. [PubMed: 16096063]
12. Moiseyev G, Chen Y, Takahashi Y, Wu BX, Ma JX. RPE65 is the isomerohydrolase in the retinoid visual cycle. Proc Natl Acad Sci U S A 2005;102:12413–12418. [PubMed: 16116091]
13. Redmond TM, Poliakov E, Yu S, Tsai JY, Lu Z, Gentleman S. Mutation of key residues of RPE65 abolishes its enzymatic role as isomerohydrolase in the visual cycle. Proc Natl Acad Sci U S A 2005;102:13658–13663. [PubMed: 16150724]
14. Simon A, Hellman U, Wernstedt C, Eriksson U. The retinal pigment epithelial-specific 11-cis retinol dehydrogenase belongs to the family of short chain alcohol dehydrogenases. J Biol Chem 1995;270:1107–1112. [PubMed: 7836368]
15. Mata NL, Radu RA, Clemmons RC, Travis GH. Isomerization and oxidation of vitamin a in cone-dominant retinas: a novel pathway for visual-pigment regeneration in daylight. Neuron 2002;36:69–80. [PubMed: 12367507]
16. Mata NL, Ruiz A, Radu RA, Bui TV, Travis GH. Chicken retinas contain a retinoid isomerase activity that catalyzes the direct conversion of all-trans-retinol to 11-cis-retinol. Biochemistry 2005;44:11715–11721. [PubMed: 16128572]
17. Trevino SG, Villazana-Espinoza ET, Muniz A, Tsin AT. Retinoid cycles in the cone-dominated chicken retina. J Exp Biol 2005;208:4151–4157. [PubMed: 16244173]
18. Thompson DA, Gal A. Vitamin A metabolism in the retinal pigment epithelium: genes, mutations, and diseases. Prog Retin Eye Res 2003;22:683–703. [PubMed: 12892646]
19. Saari JC, Garwin GG, Van Hooser JP, Palczewski K. Reduction of all-trans-retinal limits regeneration of visual pigment in mice. Vision Res 1998;38:1325–1333. [PubMed: 9667000]
20. Saari JC, Nawrot M, Kennedy BN, et al. Visual cycle impairment in cellular retinaldehyde binding protein (CRALBP) knockout mice results in delayed dark adaptation. Neuron 2001;29:739–748. [PubMed: 11301032]
21. Maeda A, Maeda T, Imanishi Y, et al. Role of photoreceptor-specific retinol dehydrogenase in the retinoid cycle in vivo. J Biol Chem 2005;280:18822–18832. [PubMed: 15755727]

22. Ala-Laurila P, Kolesnikov AV, Crouch RK, et al. Visual cycle: Dependence of retinol production and removal on photoproduct decay and cell morphology. J Gen Physiol 2006;128:153–169. [PubMed: 16847097]
23. Chen C, Tsina E, Cornwall MC, Crouch RK, Vijayaraghavan S, Koutalos Y. Reduction of all-trans retinal to all-trans retinol in the outer segments of frog and mouse rod photoreceptors. Biophys J 2005;88:2278–2287. [PubMed: 15626704]
24. Tsina E, Chen C, Koutalos Y, Ala-Laurila P, Tsacopoulos M, Wiggert B, et al. Physiological and microfluorometric studies of reduction and clearance of retinal in bleached rod photoreceptors. J Gen Physiol 2004;124:429–443. [PubMed: 15452202]
25. Redmond TM, Yu S, Lee E, et al. Rpe65 is necessary for production of 11-cis-vitamin A in the retinal visual cycle. Nat Genet 1998;20:344–351. [PubMed: 9843205]
26. Mears AJ, Kondo M, Swain PK, et al. Nrl is required for rod photoreceptor development. Nat Genet 2001;29:447–452. [PubMed: 11694879]
27. Daniele LL, Lillo C, Lyubarsky AL, et al. Cone-like morphological, molecular, and electrophysiological features of the photoreceptors of the Nrl knockout mouse. Invest Ophthalmol Vis Sci 2005;46:2156–2167. [PubMed: 15914637]
28. Okajima TL, Pepperberg DR. Retinol kinetics in the isolated retina determined by retinoid extraction and HPLC. Exp Eye Res 1997;65:331–340. [PubMed: 9299170]
29. Wu Q, Blakeley LR, Cornwall MC, Crouch RK, Wiggert BN, Koutalos Y. Interphotoreceptor retinoid-binding protein is the physiologically relevant carrier that removes retinol from rod photoreceptor outer segments. Biochemistry 2007;46:8669–8679. [PubMed: 17602665]
30. Lem J, Krasnoperova NV, Calvert PD, et al. Morphological, physiological, and biochemical changes in rhodopsin knockout mice. Proc Natl Acad Sci U S A 1999;96:736–741. [PubMed: 9892703]
31. Kolesnikov AV, Ala-Laurila P, Shukolyukov SA, et al. Visual cycle and its metabolic support in gecko photoreceptors. Vision Res 2007;47:363–374. [PubMed: 17049961]
32. Nikonov SS, Daniele LL, Zhu X, Craft CM, Swaroop A, Pugh EN Jr. Photoreceptors of $Nrl^{-/-}$ mice coexpress functional S- and Mcone opsins having distinct inactivation mechanisms. J Gen Physiol 2005;125:287–304. [PubMed: 15738050]
33. Wenzel A, von Lintig J, Oberhauser V, Tanimoto N, Grimm C, Seeliger MW. RPE65 is essential for the function of cone photoreceptors in NRL-deficient mice. Invest Ophthalmol Vis Sci 2007;48:534–542. [PubMed: 17251447]
34. Feathers KL, Lyubarsky AL, Khan NW, et al. Nrl-knockout mice deficient in Rpe65 fail to synthesize 11-cis retinal and cone outer segments. Invest Ophthalmol Vis Sci 2008;49:1126–1135. [PubMed: 18326740]
35. Matthews RG, Hubbard R, Brown PK, Wald G. Tautomeric forms of metarhodopsin. J Gen Physiol 1963;47:215–240. [PubMed: 14080814]
36. Dukkipati A, Kusnetzow A, Babu KR, et al. Phototransduction by vertebrate ultraviolet visual pigments: protonation of the retinylidene Schiff base following photobleaching. Biochemistry 2002;41:9842–9851. [PubMed: 12146950]
37. Bowmaker JK, Dartnall HJ, Lythgoe JN, Mollon JD. The visual pigments of rods and cones in the rhesus monkey, Macaca mulatta. J Physiol 1978;274:329–348. [PubMed: 415133]
38. Wenzel A, Reme CE, Williams TP, Hafezi F, Grimm C. The Rpe65 Leu450Met variation increases retinal resistance against light-induced degeneration by slowing rhodopsin regeneration. J Neurosci 2001;21:53–58. [PubMed: 11150319]
39. Lyubarsky AL, Savchenko AB, Morocco SB, Daniele LL, Redmond TM, Pugh EN Jr. Mole quantity of RPE65 and its productivity in the generation of 11-cis-retinal from retinyl esters in the living mouse eye. Biochemistry 2005;44:9880–9888. [PubMed: 16026160]
40. Heck M, Schadel SA, Maretzki D, et al. Signaling states of rhodopsin. Formation of the storage form, metarhodopsin III, from active metarhodopsin II. J Biol Chem 2003;278:3162–3169. [PubMed: 12427735]
41. Sommer ME, Smith WC, Farrens DL. Dynamics of arrestin-rhodopsin interactions: arrestin and retinal release are directly linked events. J Biol Chem 2005;280:6861–6871. [PubMed: 15591052]

42. Sun H, Molday RS, Nathans J. Retinal stimulates ATP hydrolysis by purified and reconstituted ABCR, the photoreceptor-specific ATP-binding cassette transporter responsible for Stargardt disease. J Biol Chem 1999;274:8269–8281. [PubMed: 10075733]

43. Beharry S, Zhong M, Molday RS. N-retinylidene-phosphatidylethanolamine is the preferred retinoid substrate for the photoreceptor-specific ABC transporter ABCA4 (ABCR). J Biol Chem 2004;279:53972–53979. [PubMed: 15471866]

44. Weng J, Mata NL, Azarian SM, Tzekov RT, Birch DG, Travis GH. Insights into the function of Rim protein in photoreceptors and etiology of Stargardt's disease from the phenotype in abcr knockout mice. Cell 1999;98:13–23. [PubMed: 10412977]

45. Kusnetzow AK, Dukkipati A, Babu KR, Ramos L, Knox BE, Birge RR. Vertebrate ultraviolet visual pigments: protonation of the retinylidene Schiff base and a counterion switch during photoactivation. Proc Natl Acad Sci U S A 2004;101:941–946. [PubMed: 14732701]

46. Miyazono S, Shimauchi-Matsukawa Y, Tachibanaki S, Kawamura S. Highly efficient retinal metabolism in cones. Proc Natl Acad Sci U S A 2008;105:16051–16056. [PubMed: 18836074]

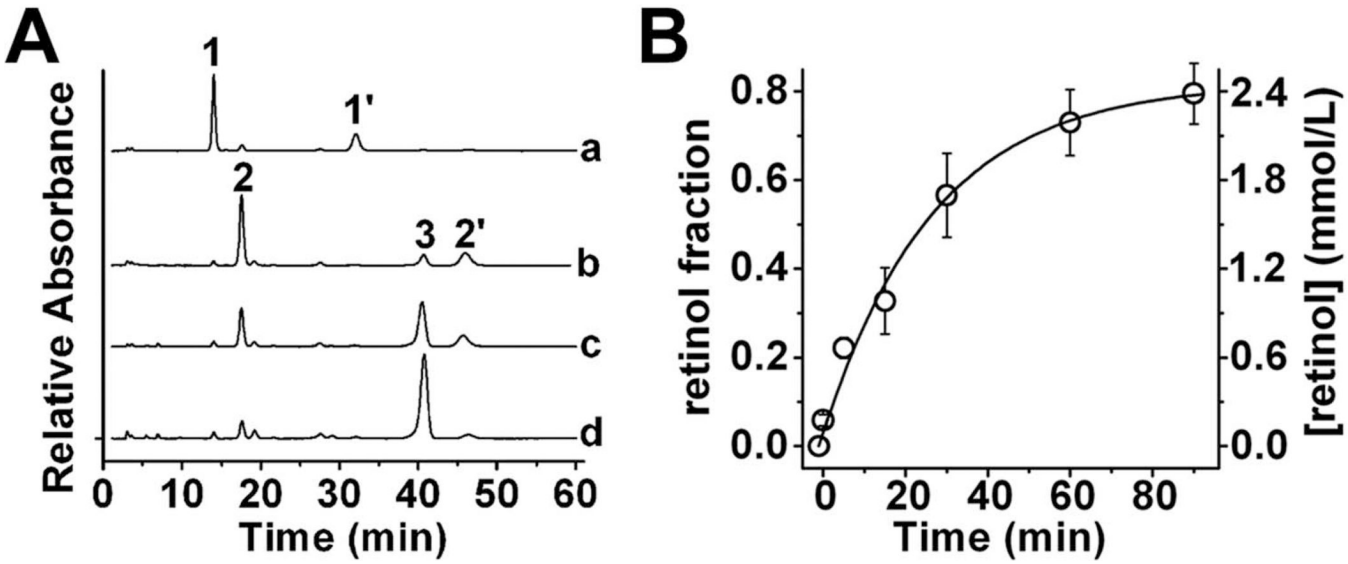

Figure 1.

Formation of all-*trans* retinol in retinas of wild-type mice. (**A**) Chromatograms (at 325 nm) of retinoid extractions from wild-type mouse retinas, incubated for different times after bleaching at 37°C: *trace a*, dark control; *trace b*, immediately after bleaching; *trace c*, 15 minutes after bleaching; and *trace d*, 60 minutes after bleaching. 1, *syn*-11-*cis* retinal oxime; 1′, *anti*-11-*cis* retinal oxime; 2, *syn*-all-*trans* retinal oxime; 2′, *anti*-all-*trans* retinal oxime; and 3, all-*trans* retinol. To facilitate comparisons, the traces have been normalized to the total amount of retinoid present in each sample. (**B**) Kinetics of all-*trans* retinol formation after bleaching as measured from experiments such as the ones shown in (**A**). Each point is the average of at least four experimental determinations; error bars, SD. Bleaching was performed between $t = -1$ minute and $t = 0$. The curve is a single exponential least-squares fit (equation 2; $R = 0.99$) giving $f_1 = 0.04$ minute^{-1}.

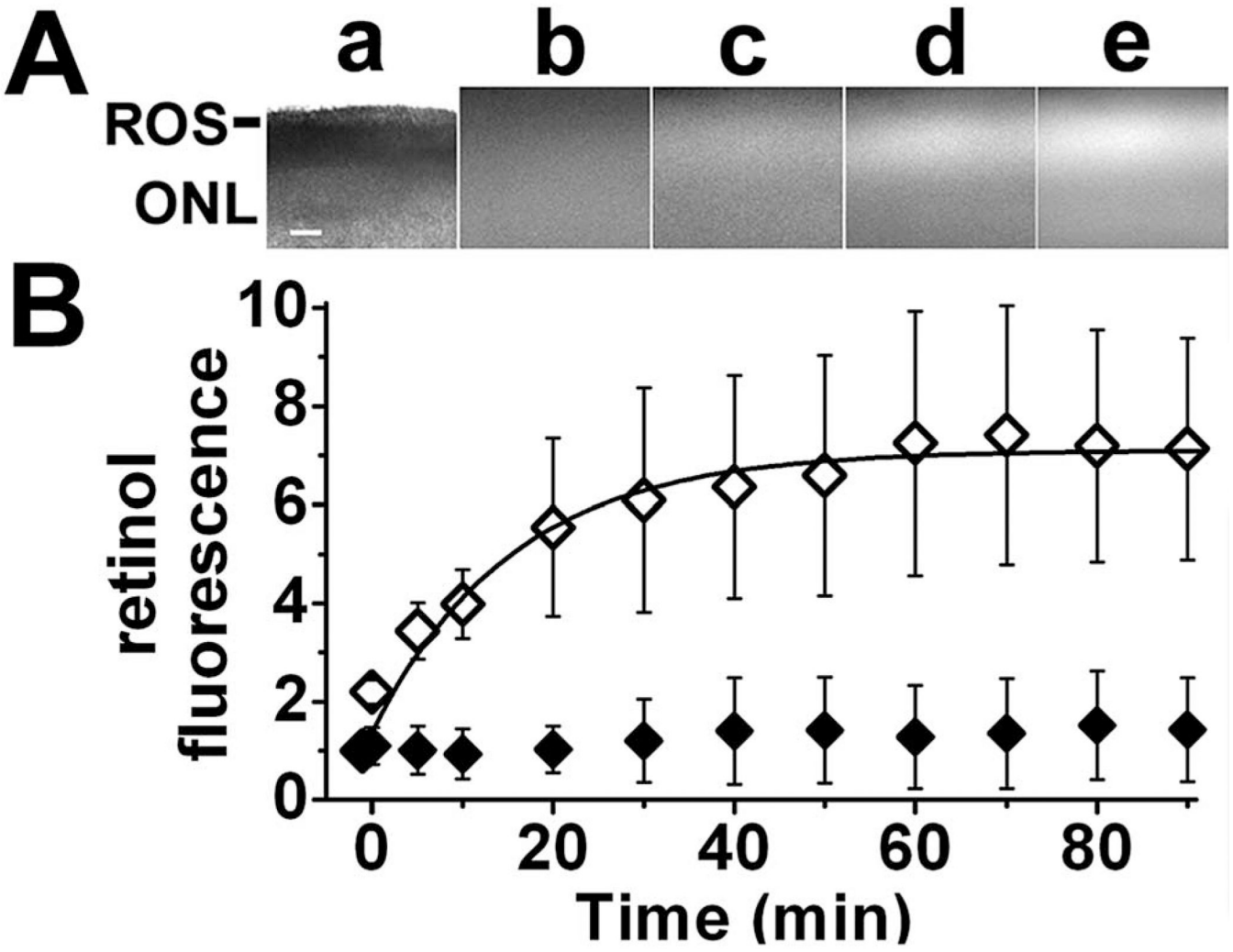

Figure 2.

Formation of all-*trans* retinol in biochemically active retina slices. (**A**) Retinol fluorescence increased in the rod outer segment layer after rhodopsin bleaching. (**Aa**) Infrared image of the photoreceptor layer of the unbleached retina slice. (**Ab–e**) Fluorescence (excitation, 360 nm; emission, >420 nm) images of the photoreceptor layer (**Ab**) before bleaching, (**Ac**) immediately after bleaching, and (**Ad**) 10 and (**Ae**) 90 minutes after bleaching. Fluorescence images are shown at different intensity scalings. Experiment was conducted at 37°C. Bar, 20 μm. (**B**) Kinetics of all-*trans* retinol formation after bleaching for wild-type mice (◊, $n = 8$). There was no significant fluorescence increase in the rod outer segments of *Rpe65*$^{-/-}$ mice (♦, $n = 7$). In all experiments, the first time point (at $t = -1$ minute) was the outer segment fluorescence of the dark-adapted slice, and all subsequent fluorescence values were normalized to that one. Error bars, SD. Bleaching was performed between $t = -1$ minute and $t = 0$. The curve is a single exponential least-squares fit ($R = 0.99$; equation 2) to the wild-type data, giving $f_1 = 0.06$ minute^{-1}.

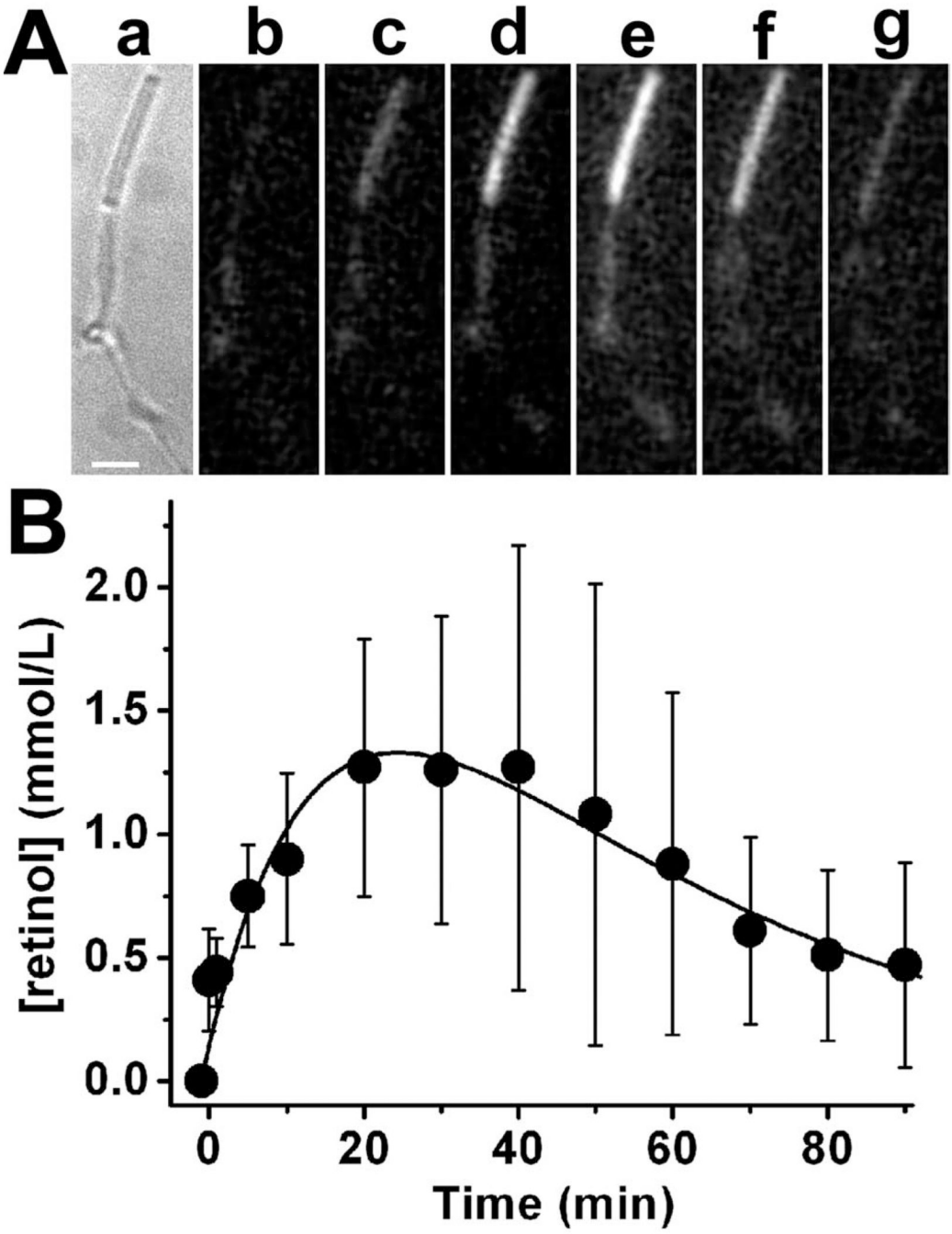

Figure 3.

Formation of all-*trans* retinol in isolated rod photoreceptors from wild-type mice. (**A**) Retinol fluorescence increased in the rod outer segment after rhodopsin bleaching. (**Aa**) infrared image of an intact isolated rod photoreceptor. (**Ab–g**) Fluorescence (excitation, 360 nm; emission, >420 nm) images of the cell (**Ab**) before bleaching, (**Ac**) immediately after bleaching, and (**Ad**) 10, (**Ae**) 20, (**Af**) 30, and (**Ag**) 60 minutes after bleaching. All fluorescence images are shown at the same intensity scaling. Experiment performed at 37°C. Bar, 5 μm. Fluorescence intensities were converted to retinol concentrations after calibration with hexane/chloroform droplets containing a known concentration of retinol. (**B**) Rod outer segment all-*trans* retinol concentration at different times after bleaching of the outer segment complement of rhodopsin

(n = 13 cells). Error bars, SD. Bleaching was performed between $t = -1$ minute and $t = 0$. The curve is least-squares fit of equation 4 to the data ($R = 0.96$) giving $f_1 = 0.06$ minute^{-1}, $f_2 = 0.024$ minute^{-1}, and $C_0 = 2.5$ mM.

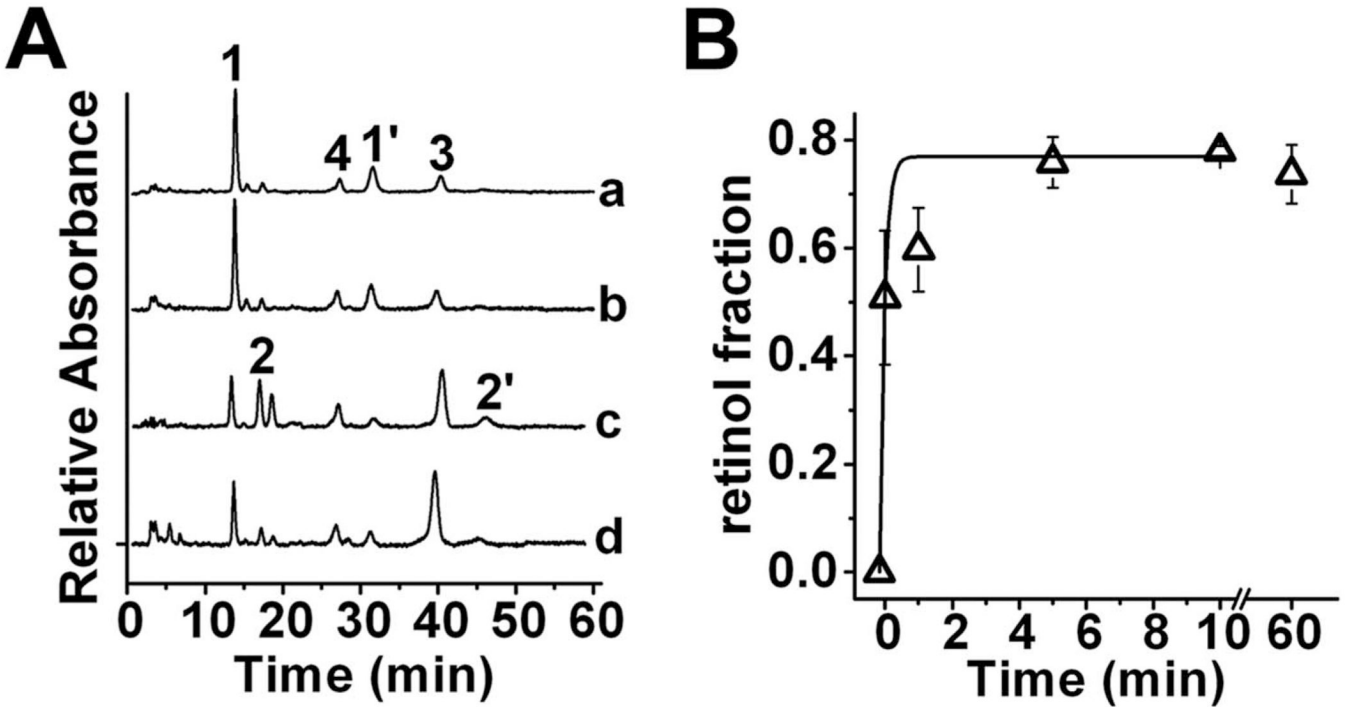

Figure 4.

all-*trans* retinol formation in retinas of $Nrl^{-/-}$ mice. (**A**) Chromatograms (at 325 nm) of retinoid extractions from $Nrl^{-/-}$ mouse retinas, incubated for different times after bleaching at 37°C; *trace a*, dark control; *trace b*, immediately after bleaching with long wavelength (>530 nm) light; *trace c*, immediately after bleaching with UV (360 nm) light; *trace d*, 5 minutes after bleaching with UV light. 1, *syn*-11-*cis* retinal oxime; 1′, *anti*-11-*cis* retinal oxime; 2, *syn*-all-*trans* retinal oxime; 2′, anti-all-*trans* retinal oxime; 3, all-*trans* retinol; and 4, 11-*cis* retinol. (**B**) Kinetics of all-*trans* retinol formation after bleaching as measured from experiments like the ones shown in (**A**). Each point is the average of at least four experimental determinations. Error bars, SD. Bleaching was performed between $t = -10$ seconds and $t = 0$. The curve is a single exponential least squares fit ($R = 0.97$; equation 2) giving $f_1 = 6.8$ minutes^{-1}.

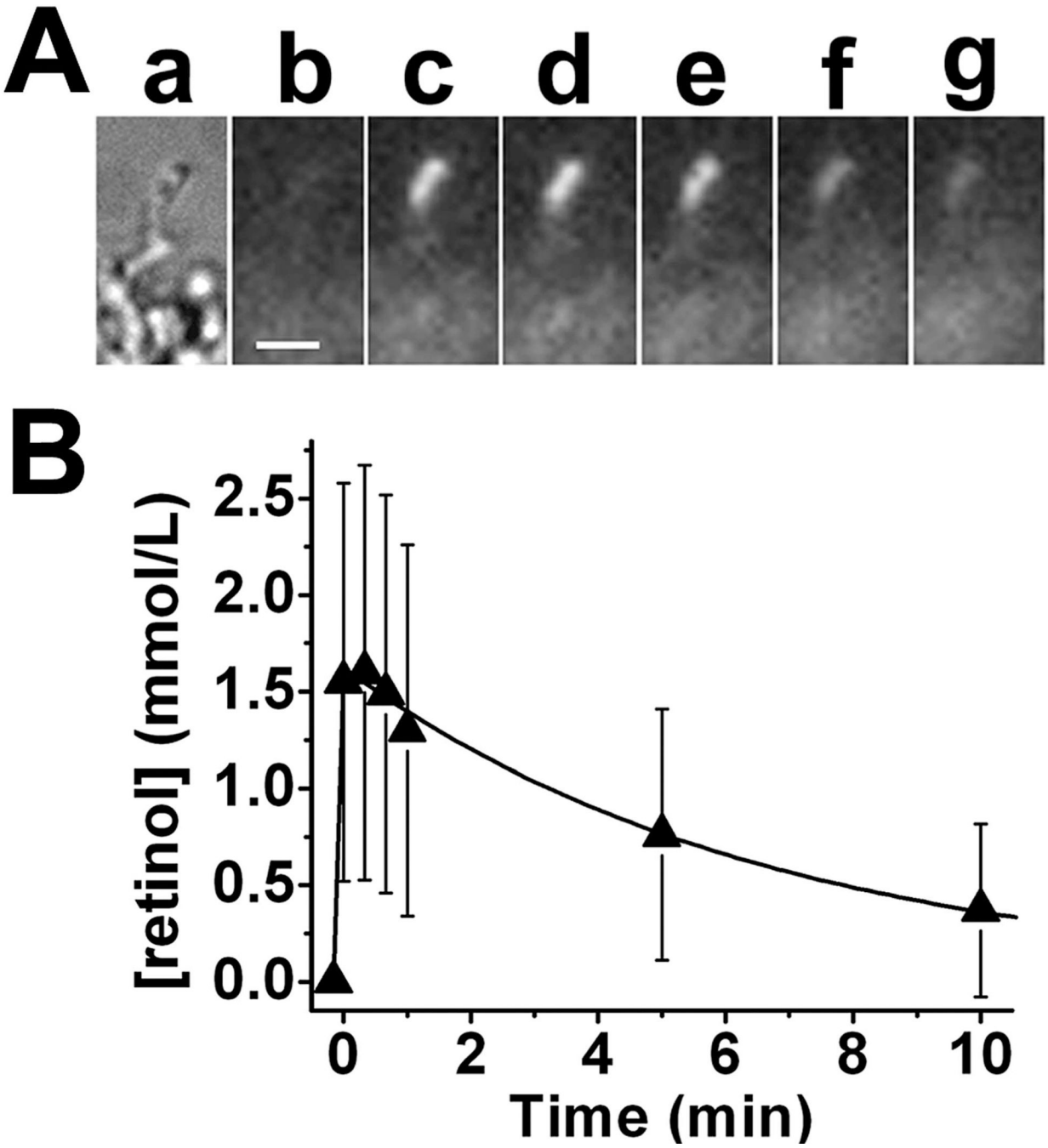

Figure 5.

Formation of all-*trans* retinol in a single photoreceptor from *Nrl*$^{-/-}$ mice. (**A**) Fluorescence increased in this outer segment of a single photoreceptor after visual pigment bleaching. (**Aa**) Infrared image of an intact cell. (**Ab–g**) Fluorescence (excitation, 360 nm; emission, >420 nm) images of the cell (**Ab**) before bleaching, (**Ac**) immediately after bleaching, and (**Ad**) 20 seconds, (**Ae**) 60 seconds, (**Af**) **5** minutes, and (**Ag**) 10 minutes after bleaching. All fluorescence images are shown at the same intensity scaling. Experiment performed at 37°C. Bar, 5 μm. Fluorescence intensities were converted to retinol concentrations after calibration with hexane/chloroform droplets containing a known concentration of retinol. (**B**) Outer segment all-*trans* retinol concentration at different times after bleaching (n = 6 cells). Error bars, SD.

Bleaching was performed between $t = -10$ seconds and $t = 0$. The curve is the least-squares fit of equation 4 to the data ($R = 0.99$), giving $f_1 = 19.5$ minutes^{-1}, $f_2 = 0.15$ minute^{-1}, and $C_0 = 1.7$ mM.